Hindawi Publishing Corporation
Journal of Mining
Volume 2015, Article ID 235636, 9 pages
http://dx.doi.org/10.1155/2015/235636

Research Article

Laboratory Studies of Electric Current Generated during Fracture of Coal and Rock in Rock Burst Coal Mine

Zhonghui Li, Enyuan Wang, and Miao He

Faculty of Safety Engineering, China University of Mining and Technology, Xuzhou, Jiangsu 221116, China

Correspondence should be addressed to Zhonghui Li; lizhonghui@cumt.edu.cn

Received 29 August 2014; Revised 26 January 2015; Accepted 2 February 2015

Academic Editor: Luigi Toro

Experiments show that electric current would be produced in uniaxial compression of coal and roof rock. The electric current of coal shows a rapid increasing tendency when the loading stress is greater than or equal to $0.75\sigma_{max}$ which can be regarded as an omen for coal failure. The current of roof rock shows reversal tendency while loading stress is greater than or equal to $0.91\sigma_{max}$ and revised from negative to positive at the main fracture and the reversal of current can be regarded as the omen of rock fracture. There are obvious differences in physical and mechanical properties, composition, and failure process between coal and rock. The dominant mechanism of electric current generated by coal is triboelectrification of coal particles and charge separation during crack propagation. The mechanism of electric current of roof rock is piezoelectric effect of quartz materials in the early stage and charge separation during crack propagation in the later stage of loading. It can be found that the rapid increasing and reversal characteristic of electric current can reflect the failure process of coal and roof rock, respectively. Thus, it can be considered the omen of coal and rock failure.

1. Introduction

As we all know, China is the world's largest coal producer and consumer. As a result, China is one of the countries suffering from such coal-mine disasters as rock burst as well as coal and gas outburst [1–3]. With the mining depth of coal mines in China extending deep vertically at the annual speed of 10–20 m (the fastest is 50 m), the ground stress, gas pressure, and gas content of coal seam increase gradually. Besides, the complicated geological structure of coal mines in China makes the disasters in coal mines extremely severe [4, 5]. Coal and rock disaster refers to the process of sudden unstability or failure occurring as a result of deformation and fracture of coal or rock under the influence of ground stress and mining-induced stress. Such events are always accompanied by loud sound, vibration, and coal or rock bump, which have caused serious destruction and threaten the safety of mine and personnel safety [3]. A failure caused by rock burst is shown in Figure 1.

During the process of coal and rock dynamic disaster, different energies are dissipated in the form of elastic energy, heat, acoustic energy, and electromagnetic energy. A number of studies have shown that electromagnetic radiation signal will be generated during coal compression failure in laboratory and damage of coal seam in mines [6–8]. In addition, electromagnetic radiation technology has been applied to the monitoring and prediction of rock burst and coal and gas outburst in coal mines [9–12]. With regard to the prediction of earthquakes and volcano eruptions, a number of experiments were conducted on electrical anomaly of marble and granite fracture process. The results of such studies have been used for monitoring earthquake and volcano activities, and so forth. Some experimental results have also shown that positive charge is generated on the granite surface under uniaxial compression [13]. In addition, free charges are generated when marble is compressed. The amount of charges generated increases sharply during loading and unloading, but suddenly it decreases gradually [14–16]. Both granite and marble would generate negative electric potential signal during deformation and fracture under double-axial pressure and uniaxial pressure. In addition, the variation of electric potential has good congruity with the sudden change of

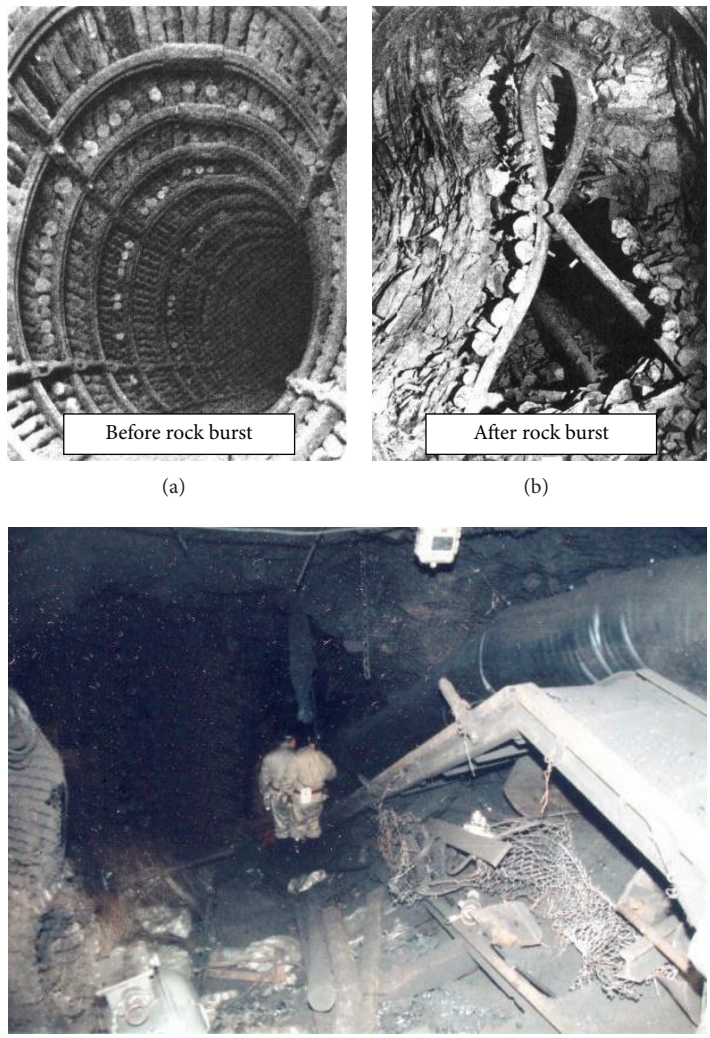

Figure 1: Rock burst disaster: (a) tunnel before rock burst, (b) damaged tunnel after rock burst, and (c) damaged equipment.

stress [17, 18]. Precursory electric potential signals before failure were observed in both saturated and dry samples of the quartz-rich sandstones but only observed in the water-saturated quartz-free limestone [19]. Water flowing in fractured rock mass will produce direct current and electric potential signal [20]. The marble under uniaxial compression stress would produce electric current during fracture under load. The electric current is relevant to the change of Young modulus of rock samples and there is a certain proportionality between electric current peak and stress ratio [21]. The precursory change of electrical signal has been tested before the stick-slip process in friction experiments of piezoelectric quartz and nonpiezoelectric gabbroic gouges [22]. During quick loading on granite and gabbro, electric current of about 35 pA and instant potential of about 40 mV can be obtained [23]. Some authors performed uniaxial cyclic loading on granite samples ($69.6 \times 49.0 \times 51.2$ mm) and then calculated the decrease in electric current peak intensity progressively in proper order [24]. When two electric currents with opposite polarity and same magnitude were tested in the stressed and unstressed parts of igneous rocks, the instantaneous drastic change in electric current was reported to predict crustal rock breaking ahead of an earthquake [25]. Some scholars have succeeded in forecasting strong earthquake by testing vertical component in underground electric fields [26–29].

Compared with such seismogenic rocks as granite and marble, coal and coal-measure rocks have different components and properties that contain a large number of macrojoints and microfissures as well as lower compression strength. Therefore, can coal and coal-measure rocks generate electric current during compression fracture process? In addition, what kind of rules does it have? To investigate how electric currents are associated with fracture of coal and rock, experiment studies were conducted on electric currents of coal and rock under uniaxial compression using electric current experiment system. The correlation between current

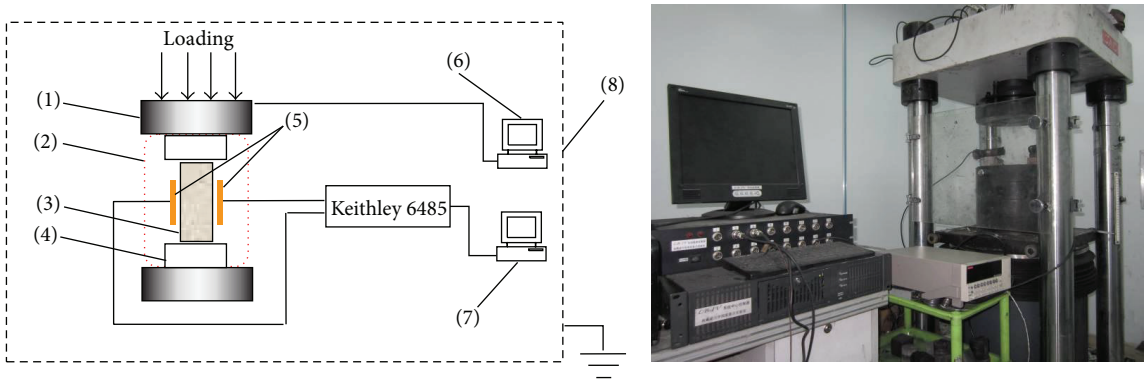

(1) Testing machine
(2) Shielding net
(3) Coal and rock samples
(4) Insulation block
(5) Electrode
(6) Loading control system
(7) Electric current data collecting system
(8) Electromagnetic shielding room

(a) (b)

FIGURE 2: Experimental system used for studying electric current generated during coal and rock fracture. (a) Schematic diagram of the setup. (b) Photo of the experimental system.

and stress and the generation mechanism of current were studied and analyzed. These findings provide some technical means for monitoring coal-rock failure process of coal mines.

2. Experimental Studies

2.1. Experiment System and Sample Preparation. The experiments in this study are conducted in GP6-type electromagnetic shielding room in China University of Mining and Technology. The shielding effect is above 85 dB, which can effectively reduce electromagnetic interference from devices such as electrical power system, radio broadcast, and communication radio. The testing system includes a loading system, electric current data collecting system, electrode, and shielding net. As shown in Figure 2, the loading system is computer-controlled SANS YAW-4306 electrohydraulic servo compression-testing machine, which has several functions including stress closed-loop control, constant stress control, constant strain control, and load holding. The electric current data collecting system is composed of Keithley 6485-type picoammeter and control computer. This picoammeter has high, medium, and low sampling rates with measurement range of ±20 fA to ±21 mA. The electrode used in the experiment is copper electrode (size, 15 × 15 mm).

The coal samples in this experiment were chosen from the Changgouyu coal mine in Beijing. The mine is one of those with a high risk of rock burst. The samples were processed into 50 × 100 mm cylinders using raw coal and roof rock with a core barrel and smoothed at both ends. Figure 2 shows this processing; the cylinder was dried under normal room temperature to allow it to dry normally.

2.2. Layout of Testing Point. Copper electrodes were placed in a symmetrical position on both sides of the sample.

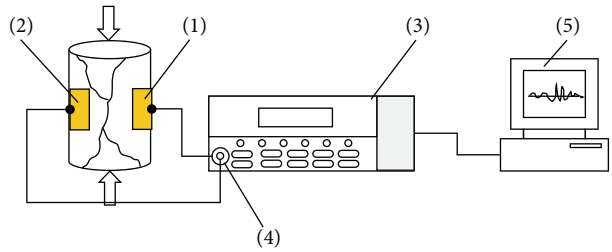

(1, 2) Electrode
(3) Picoammeter
(4) Input terminal
(5) Data acquisition and control computer

FIGURE 3: Diagram of testing point layout.

The electrodes connect into the "HI" and "LO" terminals of the picoammeter. The current generated by coal and rock failure is tested by the picoammeter through the electrode and the data are stored by the control computer; see Figure 3.

2.3. Experimental Procedures. First, the copper electrode is pasted on both sides of the samples in a symmetric position using a conductive adhesive and then stored in normal temperature for a while until it reaches poling stability.

Second, start the Keithley 6485 picoammeter in order for it to warm up and select the testing parameters. Then connect the picoammeter to the control computer.

Third, put the samples on the piston of testing machine and fill up the insulation block (Epoxy glass fabric laminate) at both ends. Then, connect the electrode with the picoammeter input cable.

Fourth, start the test machine and picoammeter control computer in synchronization for electric current and stress data acquisition.

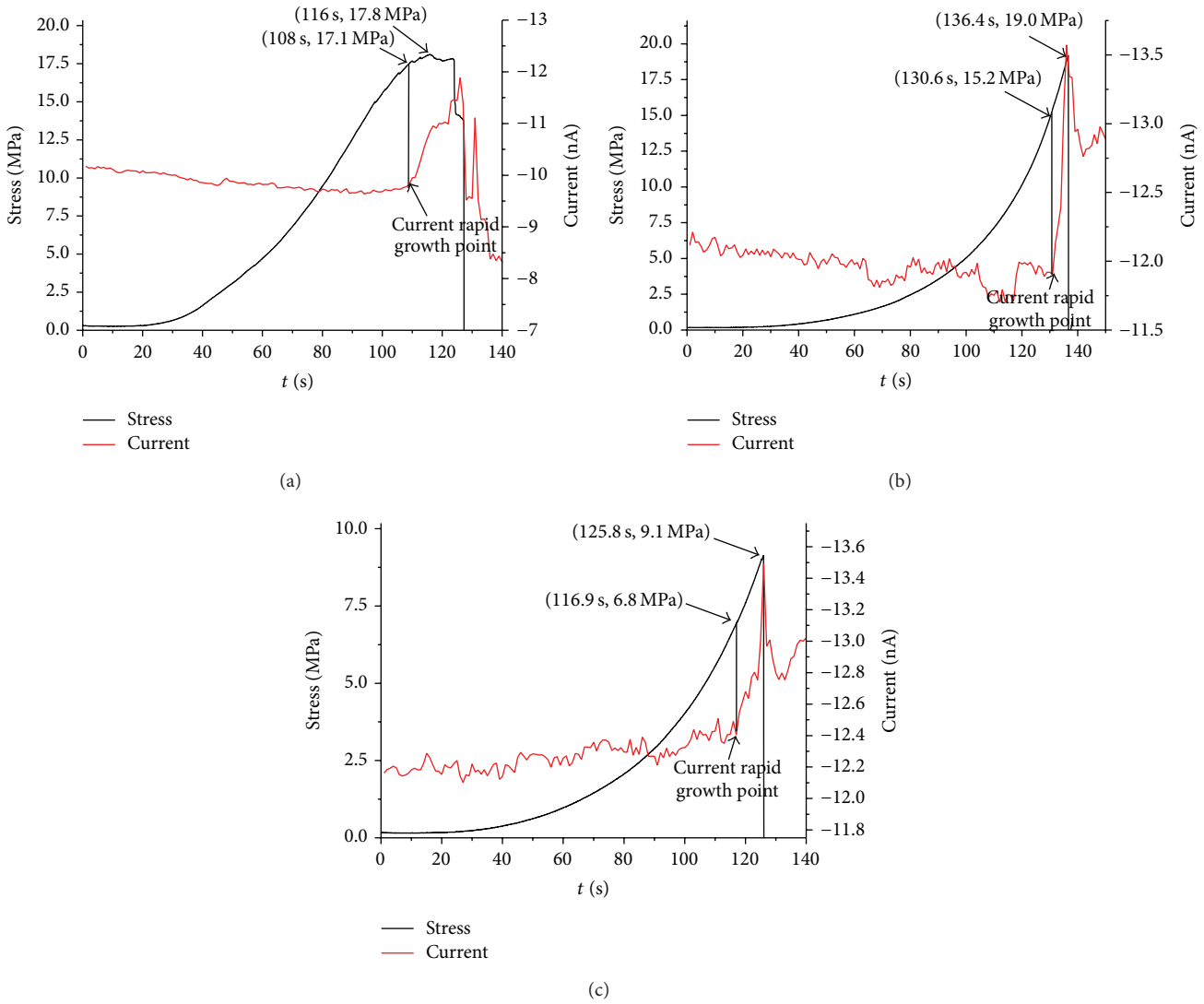

Figure 4: Electric current of coal samples under uniaxial compression. (a) Coal sample number 1, (b) coal sample number 2, and (c) coal sample number 3.

Fifth, stop loading and electric current data acquisition after the coal and rock samples have fractured.

3. Experiment Results and Explanation

3.1. Electric Current of Coal Samples under Uniaxial Compression. In this experiment, 15 coal samples were selected. The coal samples were then loaded under uniaxial compression in constant strain increase mode at the speed of 0.2 mm/min on the testing machine. The three representative results were analyzed, as shown in Figure 4(a) to Figure 4(c). Electric current would be generated during the process of compression failure. The current increases along with the increase in stress before peak stress is reached. During this process, current shows a tendency of rapid growth before main fracture of the samples and reaches the maximum value at the main fracture of the samples. As shown in Figure 4(a), in the compaction and elastic deformation stage of coal sample loading, there is little electric current variation (about −10 nA). When coal samples begin plastic deformation (108 s, 17.1 MPa), the current increases rapidly along with loading. When the loading stress reaches the maximum value (116 s, 17.8 MPa), the current is about −11 nA (1 nA = 10^{-9} A). Once peak stress is reached, the samples enter into an unstable failure stage. At 127 s, there is complete failure in samples with instantaneous current peak reaching −11.9 nA. Both Figures 4(b) and 4(c) show similar regularities, and there is rapid increase in current in the plastic deformation stage of coal samples. The rapid increase of current is shown in Figure 4(b), (130.6 s, 15.2 MPa), and Figure 4(c), (116.9 s, 6.82 MPa). Experimental results show that electric current generated during coal sample failure has good consistency with the stress received. Besides, the change in electric current reflects the failure state of coal samples.

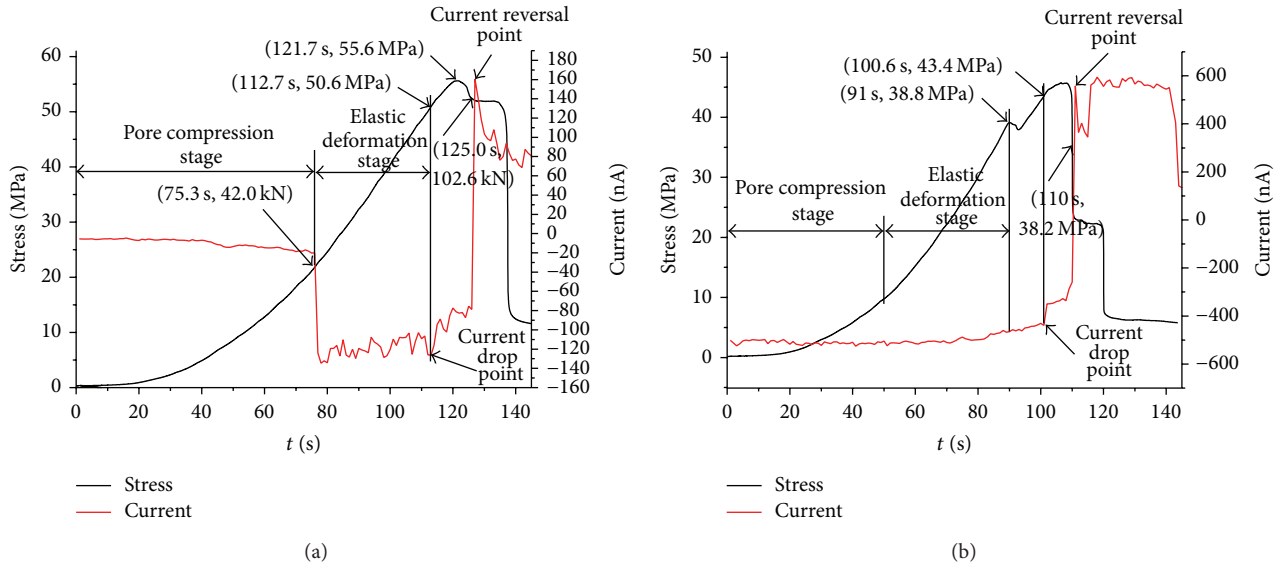

FIGURE 5: Electric current of roof rock samples under uniaxial compression: (a) roof rock sample number 1 and (b) roof rock sample number 2.

3.2. Electric Current of Roof Rock under Uniaxial Compression. Five sets of experiments were conducted to study the electric current of roof rock samples under uniaxial compression with the loading speed of 0.2 mm/min. Results of these experiments indicate that the electric current generated by roof rock is very much different from that of coal, as an alternating pattern of current flow is noted and the direction reversal of the electric current is related to the destruction process of rock.

As shown in Figure 5(a), the electric current is stable with little change in the early loading stage. When loading at the moment of 75.3 s, the stress is 21.4 MPa, and the rock samples enter into the elastic deformation stage while reaching 38.5% of σ_{max}. In this case, the value of electric current generated instantaneously is −134.6 nA. When continuing loading at the moment of 112.7 s, the stress is 50.6 MPa. The rock samples at this scenario enter into the elastic-plastic deformation stage while reaching 91% of σ_{max}. Certain quantities of newly born cracks are generated inside the samples. The free charge generated involves changes in the distribution of current between the two electrodes, leading to decreases in current amplitude to a certain degree. When loading at the moment of 121.7 s, the stress reaches the maximum of 55.6 MPa. During this point, the samples are about to enter into the main failure stage. When loading at the moment of 125.0 s, the postpeak stress is 52.2 MPa, and the samples generate a great deal of free charges by fast destruction while reaching 94% of σ_{max}. The current direction reverses from being negative to positive instantaneously with the amplitude of +160.7 nA.

As shown in Figure 5(b), the electric current at the early loading and elastic deformation stage is about −500 nA. When loading at the moment of 91 s, the stress is 38.8 MPa (i.e., 85% of σ_{max}), and the distribution of free charges generated at the two electrodes is contrary to that of former, which slightly reduces the current intensity. Later on, along with the continuous increase of loading stress, the stress is 43.4 MPa, 95% of σ_{max}, when loading at the moment of 100.6 s, and reversal of current direction occurs. In addition, the postpeak stress is 38.2 MPa at the moment of 110 s (84% of σ_{max}), and the samples fractured completely and the current intensity produced is about +557 nA.

3.3. Electric Current Characteristic Analysis

3.3.1. Electric Current of Coal Samples. Experimental results show that the electric current of coal is lower at the early loading stage but improves significantly after entering into the elastic-plastic deformation stage.

Given the stress value when electric current begins to rise rapidly

$$\sigma_c = k_c \sigma_{max}, \quad (1)$$

where k_c is stress proportionality coefficient and σ_{max} is the ultimate strength of coal sample. The character stress of coal samples under uniaxial compression and the relevance between stress and current are presented in Table 1. In the experimental analysis, when k_c increases from 0.75 to 0.94, coal samples enter into the elastic-plastic deformation and new cracks start to develop, generating a great deal of free charges. This causes a rapid rise in electric current. The value of k_c is related to such mechanical properties as coal joint and fissure development. The correlation coefficient r between electric current and stress reaches up to 0.8-0.9 before stress peak of coal samples. Therefore, the sudden increase of electric current before peak stress can be used as a precursory factor for predicting coal fracture.

3.3.2. Electric Current of Roof Rock. During roof rock compression failure, reversal of current direction is observed.

Table 1: Value of k_c during quick rising of electric current and the correlation coefficient r of coal sample.

Sample number	Time (s)	σ_c (MPa)	σ_{max} (MPa)	Proportionality coefficient k_c	Correlation coefficient r
Coal sample number 1	108.0	17.1	18.1	0.94	0.88
Coal sample number 2	130.6	15.2	19.0	0.80	0.96
Coal sample number 3	116.9	6.8	17.9	0.75	0.87

Table 2: Stress parameters corresponding to drop in amplitude and current reversal in rock samples.

	Electric current drop point (prepeak)				Electric current reversal point (postpeak)		
	Time (s)	σ_R (MPa)	σ_{max} (MPa)	Proportionality coefficient k_R	Time (s)	σ'_R (MPa)	Proportionality coefficient k'_R
Rock sample number 1	112.7	50.7	55.6	91%	125.0	52.2	94%
Rock sample number 2	100.6	43.4	45.7	95%	110.0	38.2	84%

The current shows instantaneous reversal from being negative to positive at the unstable failure stage after stress peak.

Given the stress of current amplitude drop point is σ_R and the stress of current reversal is σ'_R

$$\sigma_R = k_R \sigma_{max}\,(\text{prepeak}),$$
$$\sigma'_R = k'_R \sigma_{max}\,(\text{postpeak}), \tag{2}$$

where k_R is stress proportionality coefficient when current drops, k'_R is stress proportionality coefficient when current reverses, and σ_{max} is the ultimate strength of rock.

The parameters of the rock fracture process are presented in Table 2. It can be seen that the negative electric current starts to reduce after the samples enter into the elastic-plastic deformation stage before the peak stress. At this moment, the stress proportionality coefficient k_R changes from 0.91 to 0.95. In the fracture process after peak stress, the current direction is suddenly reversed. At this moment, the stress proportionality coefficient k'_R changes from 0.84 to 0.94.

4. Theoretical Discussion of Mechanism of Electric Current Generation from Coal and Rock

The causes of electric current generated by coal and rock failure are relevant to deformation and fracture process, physical properties, and components of coal and rock.

4.1. Analysis of Coal and Rock Composition. The components of coal and rock were tested with D/Max-3B-Type X-ray diffractometer (Rigaku Company). As shown in Figure 6, the coal consists of a small amount of kaolinite and other minerals. The roof rock is mainly composed of quartz. Meanwhile, it also contains a small quantity of feldspar, illite, montmorillonite, dolomite, calcite, and so forth. The components of coal and rock determine their mechanical properties and fracture features. Some components with piezoelectric effect have significant impact on the generation of free charges.

4.2. Analysis of Mechanism of Electric Current Generation. Being a kind of organic rock, coal has a very complicated structure and contains many cavities, point defects [29], crack defects, and minerals. As shown in Figure 6(a), coal is mainly composed of amorphous carbon, a small quantity of kaolinite, and trace amounts of other minerals. At the elastic deformation stage, the slippage and friction among grains and cracks in the coal samples can produce a great deal of free charges. The triboelectrification is the leading mechanism that is responsible for producing free charges at this stage. A large number of microfractures are formed in coal samples after they enter into the elastic-plastic and failure stages. The crack propagation destroys the chemical bonds between atoms at crack front and the charge separation at crack surfaces produces a large amount of free charges. Therefore, the dominant mechanisms responsible for production of free charges and electric current are triboelectrification and charge separation during crack propagation in the deformation and fracture process of coal [17, 30, 31].

As shown in Figure 6(b), the main component of roof rock is quartz. Two primary mechanisms are responsible for electric current generation at different failure stages. The piezoelectric effect of quartz plays a leading role in generation of free charges in the early period of loading [19, 22]. Because of heterogeneity of roof rock, the distributions of stress and fracture in different parts of samples are nonuniform during loading, which causes more accumulation of free charges at the "HI" terminal electrode than that at the "LO" terminal electrode. Thus, the "−" current occurred. At the elastic-plastic deformation stage, a large number of new cracks are produced inside the rock sample. The free charges generated by charge separation in crack propagation [31] which are accumulated at the "LO" terminal electrode are more than that at the "HI" terminal electrode. As a result, the "+" current occurred. Thus, there is reversal of current direction during the destruction process of rock.

4.3. Discussion and Analysis of Distribution of Free Charges at Different Failure Stages of Coal and Rock. Based on the aforementioned experimental results, the intensity of current produced in coal failure increases along with the increase in stress. In addition, the current of rock samples exhibits the reversal phenomenon during failure process.

As shown in Figure 4, the characteristic of electric current generated in coal fracture is relevant to the property and destruction of coal samples. At the elastic deformation

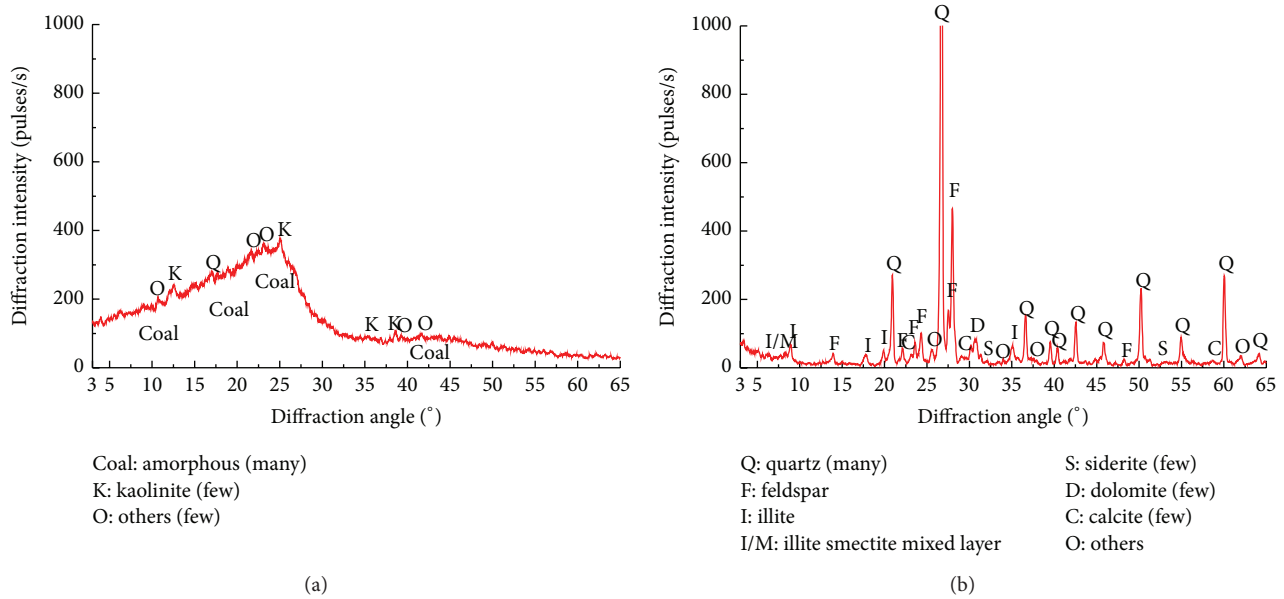

Figure 6: X-ray diffractometer curve of samples: (a) coal, (b) roof rock.

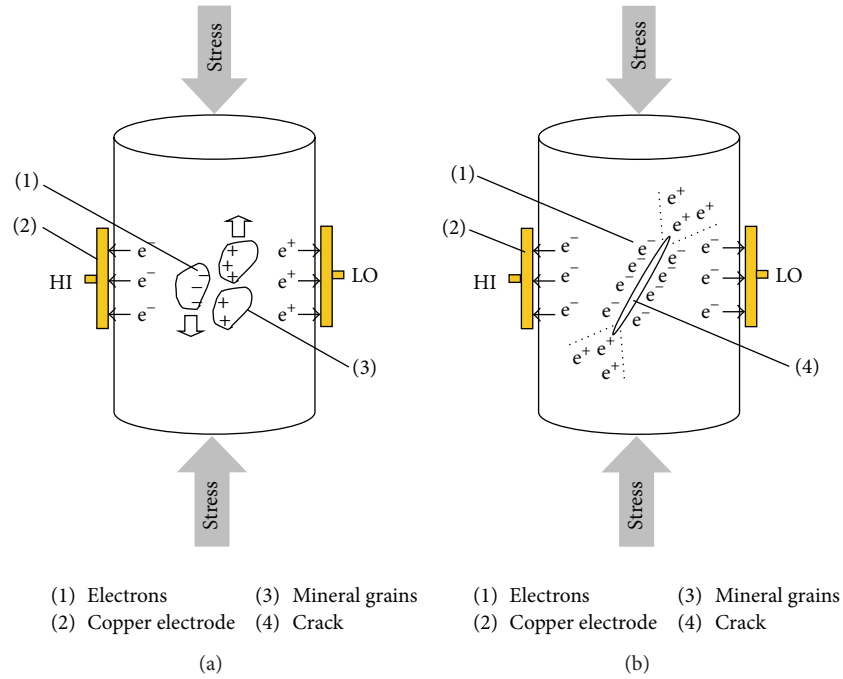

Figure 7: Distribution of free charges in different failure stages of coal: (a) elastic deformation stage and (b) elastic-plastic deformation stage.

stage, the free charges were produced by triboelectrification between mineral particles in the coal samples, as shown in Figure 7(a). As coal samples enter into the elastic-plastic deformation stage along with loading, a large number of cracks were produced gradually inside the coal samples, and large amounts of free charges were generated at both crack surfaces, as shown in Figure 7(b). The intensity of current increases along with the increases in load.

As mentioned earlier, the electric current shows the reversal phenomenon. As shown in Figure 5, this can be attributed to the mechanical process of rock failure. In the elastic deformation stage, the quartz crystal in samples produces free charges due to its piezoelectric effect. There are negative charge at the "HI" electrode and positive charge at the "LO" electrode. The current now is represented as "–." As shown in Figure 8(a), in the elastic-plastic deformation stage,

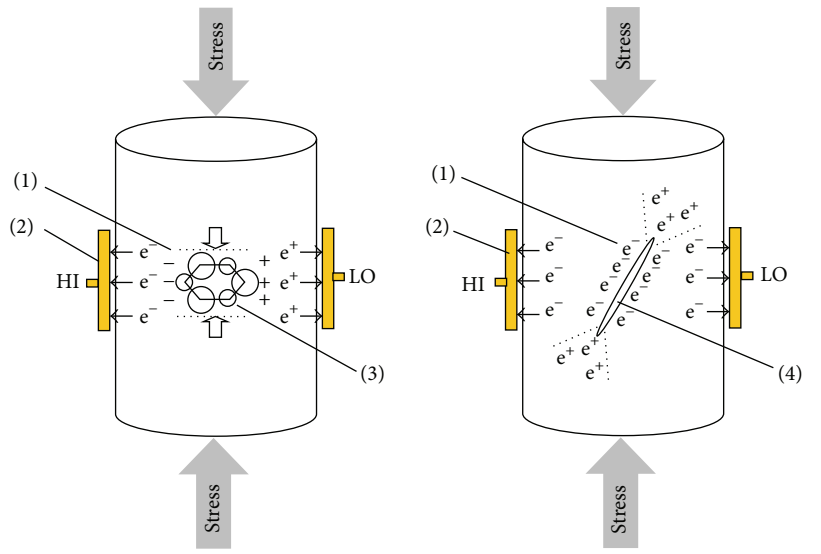

Figure 8: Distribution of free charges in different failure stage of roof rock of (a) elastic deformation stage and (b) elastic-plastic deformation stage.

large amounts of cracks were formed in rock. The free charges generated by charge separation during crack propagation accumulating at the "LO" electrode are more than that at the "HI" electrode, and this produces positive direction current as shown in Figure 8(b).

5. Conclusions

Based on the experimental results, it can be concluded that electric current will be generated during failure process of coal and rock. The electric current of coal samples has better positive correlation with stress and the rapid increasing of electric current is the precursor of coal samples fracture. The electric current of roof rock shows direction reversal from elastic deformation to plastic deformation. This phenomenon can be viewed as the precursor of rock failure. The main components of coal are amorphous carbon. Triboelectrification of particles and charge separation during crack propagation of coal samples can produce free charges, which cause electric current generation during the failure process. The different distributions of free charges produced by the piezoelectric effect and charge separation during crack propagation explain why roof rock produces electric current and there is reversal of electric current direction. The electric current of coal and rock failure reflects the fracture process of coal and rock, respectively, and provides information about the failure, which will offer a technological means for the monitoring of dynamic disasters of coal and rock.

Conflict of Interests

The authors declare that there is no conflict of interests regarding the publication of this paper.

Acknowledgments

The authors would like to acknowledge the support of The National Natural Science Foundation of China (40904028), the Foundation for the Author of National Excellent Doctoral Dissertation of PR China (201055), the Program for New Century Excellent Talents in University (NCET-10-0768), the National "Twelfth Five-Year" Plan for Science & Technology Support (2012BAK09B01, 2012BAK04B07), and the Fundamental Research Funds for the Central Universities (China University of Mining and Technology; 2011JQP06). They also thank Dr. Xiaoyan Song and Dr. Zhentang Liu for their participation in experimental test and the data analysis. They also thank all our anonymous reviewers for their useful comments and suggestions to improve the paper.

References

[1] H. He, L. Dou, J. Fan, T. Du, and X. Sun, "Deep-hole directional fracturing of thick hard roof for rockburst prevention," *Tunnelling and Underground Space Technology*, vol. 32, pp. 34–43, 2012.

[2] T. Li and M. F. Cai, "A review of mining-induced seismicity in China," *International Journal of Rock Mechanics and Mining Sciences*, vol. 44, no. 8, pp. 1149–1171, 2007.

[3] L.-M. Dou, C.-P. Lu, Z.-L. Mu, and M.-S. Gao, "Prevention and forecasting of rock burst hazards in coal mines," *Mining Science and Technology*, vol. 19, no. 5, pp. 585–591, 2009.

[4] Y. P. Cheng, H. F. Wang, L. Wang et al., *Theories and Engineering Application on Coal Mine Gas Control*, China University of Mining and Technology Press, Xuzhou, China, 2010.

[5] Y. D. Jiang, Y. X. Zhao, W. G. Liu, and J. Zhu, *Investigation on the Mechanism of Coal Bumps and Relating Experiment*, China Science Press, Beijing, China, 2009.

[6] E. Y. Wang and X. Q. He, "Experiment study on electromagnetic radiation of coal or rock during deformation and fracture," *Chinese Journal of Geophysics*, vol. 43, no. 1, pp. 131–137, 2000.

[7] V. Frid and K. Vozoff, "Electromagnetic radiation induced by mining rock failure," *International Journal of Coal Geology*, vol. 64, no. 1, pp. 57–65, 2005.

[8] V. I. Frid, A. N. Shabarov, V. M. Proskuryakov, and V. A. Baranov, "Formation of electromagnetic radiation in coal stratum," *Journal of Mining Science*, vol. 28, no. 2, pp. 139–145, 1992.

[9] V. Frid, "Rockburst hazard forecast by electromagnetic radiation excited by rock fracture," *Rock Mechanics and Rock Engineering*, vol. 30, no. 4, pp. 229–236, 1997.

[10] V. Frid, "Calculation of electromagnetic radiation criterion for rockburts hazard forecast in coal mines," *Pure and Applied Geophysics*, vol. 158, no. 5-6, pp. 931–944, 2001.

[11] V. Frid, "Electromagnetic radiation method for rock and gas outburst forecast," *Journal of Applied Geophysics*, vol. 38, no. 2, pp. 97–104, 1997.

[12] E. Wang, X. He, B. Nie, and Z. Liu, "Principle of predicting coal and gas outburst using electromagnetic emission," *Journal of China University of Mining and Technology*, vol. 29, no. 3, pp. 225–229, 2000.

[13] X. P. Wu, X. J. Shi, and Z. Q. Guo, "Study on the electrification of granite samples under compression," *Chinese Journal of Geophysics*, vol. 33, no. 2, pp. 208–211, 1990.

[14] V. S. Kuksenko and K. F. Makhmudov, "Mechanically-induced electrical effects in natural dielectrics," *Technical Physics Letters*, vol. 23, no. 2, pp. 126–127, 1997.

[15] A. Aydin, R. J. Prance, H. Prance, and C. J. Harland, "Observation of pressure stimulated voltages in rocks using an electric potential sensor," *Applied Physics Letters*, vol. 95, no. 12, Article ID 124102, 2009.

[16] I. Stavrakas, C. Anastasiadis, D. Triantis, and F. Vallianatos, "Piezo stimulated currents in marble samples: precursory and concurrent-with-failure signals," *Natural Hazards and Earth System Science*, vol. 3, no. 3-4, pp. 243–247, 2003.

[17] J. Q. Hao, L. Q. Liu, H. L. Long et al., "New result of the experiment on self-potential change of rocks under biaxial compression," *Chinese Journal of Geophysics*, vol. 47, no. 3, pp. 475–482, 2004.

[18] Y. Enomoto, T. Shimamoto, and A. Tsutumi, "Rapid electric charge fluctuation prior to rock fracturing: Its potential use for an immediate earthquake precursor," in *Proceedings of the International Workshop on Electromagnetic Phenomena Related to Earthquake Prediction*, vol. 9, pp. 64–65, 1993.

[19] D. Eccles, P. R. Sammonds, and O. C. Clint, "Laboratory studies of electrical potential during rock failure," *International Journal of Rock Mechanics and Mining Sciences*, vol. 42, no. 7-8, pp. 933–949, 2005.

[20] R. E. Nimmer, "Direct current and self-potential monitoring of an evolving plume in partially saturated fractured rock," *Journal of Hydrology*, vol. 267, no. 3, pp. 258–272, 2002.

[21] D. Triantis, I. Stavrakas, C. Anastasiadis, A. Kyriazopoulos, and F. Vallianatos, "An analysis of pressure stimulated currents (PSC), in marble samples under mechanical stress," *Physics and Chemistry of the Earth*, vol. 31, no. 4, pp. 234–239, 2006.

[22] K. Onuma, J. Muto, H. Nagahama, and K. Otsuki, "Electric potential changes associated with nucleation of stick-slip of simulated gouges," *Tectonophysics*, vol. 502, no. 3, pp. 308–314, 2011.

[23] A. Takeuchi, B. W. S. Lau, and F. T. Freund, "Current and surface potential induced by stress-activated positive holes in igneous rocks," *Physics and Chemistry of the Earth*, vol. 31, no. 4, pp. 240–247, 2006.

[24] C. Anastasiadis, D. Triantis, and C. A. Hogarth, "Comments on the phenomena underlying pressure stimulated currents in dielectric rock materials," *Journal of Materials Science*, vol. 42, no. 8, pp. 2538–2542, 2007.

[25] F. T. Freund, A. Takeuchi, and B. W. S. Lau, "Electric currents streaming out of stressed igneous rocks—a step towards understanding pre-earthquake low frequency EM emissions," *Physics and Chemistry of the Earth*, vol. 31, no. 4, pp. 389–396, 2006.

[26] P. Varotsos and M. Lazaridou, "Latest aspects of earthquake prediction in Greece based on seismic electric signals," *Tectonophysics*, vol. 188, no. 3, pp. 321–347, 1991.

[27] P. A. Varotsos, N. V. Sarlis, and E. S. Skordas, "Detrended fluctuation analysis of the magnetic and electric field variations that precede rupture," *Chaos*, vol. 19, no. 2, Article ID 023114, 2009.

[28] P. A. Varotsos, N. V. Sarlis, E. S. Skordas, and M. S. Lazaridou, "Fluctuations, under time reversal, of the natural time and the entropy distinguish similar looking electric signals of different dynamics," *Journal of Applied Physics*, vol. 103, no. 1, Article ID 014906, 2008.

[29] S. Uyeda, T. Nagao, Y. Orihara, T. Yamaguchi, and I. Takahashi, "Geoelectric potential changes: possible precursors to earthquakes in Japan," *Proceedings of the National Academy of Sciences of the United States of America*, vol. 97, no. 9, pp. 4561–4566, 2000.

[30] T. Ogawa, K. Oike, and T. Miura, "Electromagnetic radiation from rocks," *Journal of Geophysical Research*, vol. 90, no. 4, pp. 6245–6249, 1984.

[31] J. T. Dickinson, E. E. Donaldson, and M. K. Park, "The emission of electrons and positive ions from fracture of materials," *Journal of Materials Science*, vol. 16, no. 10, pp. 2897–2908, 1981.